52 *Chem. Mater.* **2010,** *22,* 52–63
DOI:10.1021/cm901514t

CHEMISTRY OF MATERIALS
Article

Synthesis, Electronic Properties, and Self-Assembly on Au{111} of Thiolated Phenylethynyl Phenothiazines

Christa S. Barkschat,[†] Svetlana Stoycheva,[‡] Michael Himmelhaus,[‡,§] and Thomas J. J. Müller*[,†]

[†]*Institut für Organische Chemie und Makromolekulare Chemie, Heinrich-Heine-Universität Düsseldorf, Universitätsstrasse 1, D-40225 Düsseldorf, Germany and* [‡]*Physikalisch-Chemisches Institut, Ruprecht-Karls-Universität Heidelberg, Im Neuenheimer Feld 253, D-69120 Heidelberg, Germany.* [§]*Present address: Research & Development Division, Fujirebio, Inc., 51 Komiya-cho, Hachioji-shi, Tokyo 192-0031, Japan.*

Received June 2, 2009. Revised Manuscript Received November 20, 2009

Thiolated phenylethynyl phenothiazines can be regarded as redox-active "alligator clips". They are readily synthesized from ethynyl phenothiazines and show intense blue-green luminescence upon ultraviolet (UV) excitation. Cyclic voltammetry reveals reversible oxidation, also after the chemisorption of in situ liberated thiols on gold electrodes. The chemisorption on Au{111} was studied by ellipsometry, contact angle measurements, X-ray photoelectron spectroscopy, and infrared reflection absorption spectroscopy, and the obtained data support the formation of self-assembled monolayers, depending on the structure of the substrates. These findings classify them as promising candidates for molecular wires switchable by redox manipulation.

Introduction

Functional organic π-systems[1] are of fundamental importance in the miniaturization of electronic devices in particular, because they could serve as molecular switches, wires, and transistors.[2] In combination with the molecule-based bottom-up approach to nanoscale structures, self-assembled monolayers (SAMs) on well-defined metal surfaces have become a ground-breaking strategy for the development of molecular electronics.[3] In recent years, many investigations of SAMs of organic molecules on gold surfaces have been conducted.[4] Thiols, thiol esters, and disulfides can be easily chemisorbed on gold to form SAMs via the exposition of well-defined gold substrates to solutions of the sulfur-functionalized molecules.[5] These "alligator clips"[6] are able to bind functional molecules covalently to Au{111} surfaces. Adsorbed on gold, phenyl derivatives,[7,8] conjugated biphenyls[7,9] and oligophenyls,[7,9,10] oligothiophenes,[7] porphyrine derivates,[9] phenanthrenes,[11] fullerenes,[12] and optically active naphthalenes[13] were studied in break junction experiments, with respect to single-molecule conductance, one-bit random access memory and, especially, as conductive molecular wires. Among the many heteroaromatic systems, phenothiazines, their derivatives, and oligomers are highly interesting building blocks for rigid-rod and wire-like molecular modules for single-molecule electronics, as a

*Author to whom correspondence should be addressed. E-mail: ThomasJJ.Mueller@uni-duesseldorf.de.

(1) For a monography, see, e.g., *Functional Organic Materials—Synthesis, Strategies, and Applications*; Müller, T. J. J., Bunz, U. H. F., Eds.; Wiley−VCH: Weinheim, Germany, 2007.
(2) (a) Timp, G. L. *Nanotechnology*; AIP Press/Springer: New York, 1999. (b) *Nanoelectronics and Information Technology: Advanced Electronic Materials and Novel Devices Information Technology*; Waser, R., Ed.; Wiley−VCH: Weinheim, Germany, 2003. (c) Joachim, C.; Gimzewski, J. K.; Aviram, A. *Nature* **2000**, *408*, 541–548. (d) Forrest, S. R. *Nature* **2004**, *428*, 911–918.
(3) Tour, J. M. *Molecular Electronics: Commercial Insights, Chemistry, Devices, Architecture and Programming*; World Scientific: River Edge, NJ, 2003.
(4) Love, J. C.; Estroff, L. A.; Kriebel, J. K.; Nuzzo, R. G.; Whitesides, G. M. Chem. Rev. **2005**, *105*, 1103−1169 and references therein.
(5) For reviews on self-assembled monolayers of thiolates on metals, see, e.g.: (a) Tao, F.; Bernasek, S. L. *Chem. Rev.* **2007**, *107*, 1408–1453. (b) Love, J. C.; Estroff, L. A.; Kriebel, J. K.; Nuzzo, R. G.; Whitesides, G. M. *Chem. Rev.* **2005**, *105*, 1103–1170. (c) Kriegisch, V.; Lambert, C. *Top. Curr. Chem.* **2005**, *258*, 257–313. (d) Otsubo, T.; Aso, Y.; Takimiya, K. *J. Mater. Chem.* **2002**, *12*, 2565–2575. (e) Ulman, A. *Acc. Chem. Res.* **2001**, *34*, 855–863. (f) Ulman, A. *Chem. Rev.* **1996**, *96*, 1533–1554. (g) Kumar, A.; Abbott, N. L.; Kim, E; Biebuyck, H. A.; Whitesides, G. M. *Acc. Chem. Res.* **1995**, *28*, 219–226.
(6) For selected examples of "alligator clips", see, e.g.: (a) Berry, J. F.; Cotton, F. A.; Murillo, C. A. *Organometallics* **2004**, *23*, 2503–2506. (b) Maya, F.; Flatt, A. K.; Stewart, M. P.; Shen, D. E.; Tour, J. M. *Chem. Mater.* **2004**, *16*, 2987–2997. (c) Seminario, J. M.; Zacarias, A. G.; Tour, J. M. *J. Am. Chem. Soc.* **1999**, *121*, 411–416. (d) Pearson, D. L.; Tour, J. M. *J. Org. Chem.* **1997**, *62*, 1376–1387.
(7) Tour, J. M.; Jones, L.II; Pearson, D. L.; Lamba, J. S.; Burgin, T.; Whitesides, G. W.; Allara, D. L.; Parikh, A. N.; Atre, S. *J. Am. Chem. Soc.* **1995**, *117*, 9529–9534.
(8) Reed, M. A.; Zhou, C.; Muller, C. J.; Burgin, T. P.; Tour, J. M. *Science* **1997**, *278*, 252–254.
(9) Tour, J. M.; Rawlett, A. M.; Kozaki, M.; Yao, Y.; Jagessar, R. C.; Dirk, S. M.; Price, D. W.; Reed, M. A.; Zhou, C.-W.; Chen, J.; Wang, W.; Campbell, I. *Chem.—Eur. J.* **2001**, *7*, 5118–5134.
(10) Bumm, L. A.; Arnold, J. J.; Cygan, M. T.; Dunbar, T. D.; Burgin, T. P.; Jones, L.II; Allara, D. L.; Tour, J. M.; Weiss, P. S. *Science* **1996**, *271*, 1705–1706.
(11) (a) Dameron, A. A.; Ciszek, J. W.; Tour, J. M.; Weiss, P. S. *J. Phys. Chem. B* **2004**, *108*, 16761–16767. (b) Ciszek, J. W.; Tour, J. M. *Tetrahedron Lett.* **2004**, *45*, 2801–2803.
(12) Shirai, Y.; Cheng, L.; Chen, B.; Tour, J. M. *J. Am. Chem. Soc.* **2006**, *128*, 13479–13489.
(13) Zhu, Y.; Gergel, N.; Majumdar, N.; Harriot, L. R.; Bean, J. C.; Pu, L. *Org. Lett.* **2006**, *8*, 355–358.

 Published on Web 12/10/2009

consequence of their electronic properties. In particular, their reversible formation of stable radical cations,[14] their tunable redox and fluorescence properties,[15] and their tendency to self-assemble on surfaces by $\pi-\pi$ interactions[16] make them eligible as redox-switchable molecular entities. However, the design of reversible phenothiazine redox systems for SAMs on gold have remained unexplored so far. In addition, the inherent folded conformation of phenothiazines,[17] with a folding angle of 158.5°, represents an intriguing new aspect for the formation of self-assembled monolayers (SAMs) of this class of compounds. Furthermore, the transformation of phenothiazines into stable planar radical cations with excellent delocalization[18] qualifies them as excellent models for switchable conductive or semiconductive molecular wires. In continuation of our studies directed to synthesize and study (oligo)phenothiazine-based functional π-systems,[19] we now have focused on thiolated phenylethynyl phenothiazines as redox-active "alligator clips". Here, we report the synthesis and their electronic properties, as studied by cyclic voltammetry (CV), as well as spectroscopic and spectrometric methods. Furthermore, to gain insight into their applicability in molecular electronics also from a practical point of view, their chemisorption and SAM formation on Au{111} was studied by ellipsometry, contact angle measurements, X-ray photoelectron spectroscopy (XPS), and infrared reflection absorption spectroscopy (IRRAS).

Experimental Section

General Remarks. All manipulations (syntheses, cyclic voltammetry, and preparations of SAMs) were conducted under an inert atmosphere of argon, and the solvents were dried by standard methods. Reagents were purchased and used without further purification, unless noted otherwise.

Column Chromatography. Silica gel 60 (Merck, Darmstadt, Germany), mesh 70−230, was used. *Thin layer chromatography* (*TLC*)*:* silica gel plates (60 F_{254}, Merck, Darmstadt, Germany). *Melting points* (*uncorrected values*)*:* Büchi melting point B-540, Stuart Scientific SMP 3, heating rate = 5 K/min; *^{1}H and ^{13}C NMR spectra:* Bruker ARX 300, Varian VXR 400S; $CDCl_3$ (locked to Me_4Si),[20] [D_6]DMSO (locked to Me_4Si). The assignments of quaternary C, CH, CH_2 and CH_3 have been made using DEPT spectra. *Infrared* (*IR*) *analysis:* Perkin−Elmer FT-IR spectrometer 1000, Bruker Vector 22. *UV/vis:* Perkin−Elmer UV/vis Spectrometer Lambda 16, Hewlett−Packard Model 8452 A. *Fluorescence spectra:* Perkin−Elmer LS 50 B (irradiation at ∼10 nm less in energy than the longest wavelength absorption maximum). *MS:* Finnigan MAT 90, Finnigan MAT 95 Q, Finnigan TSQ 700 or JEOL JMS-700. Elemental analyses were performed in the Microanalytical Laboratories of the Department Chemie, Ludwig-Maximilians-Universität München, and of the Organisch-Chemisches Institut, Ruprecht-Karls-Universität Heidelberg.

Electrochemistry. Cyclic voltammetry experiments (EG & G potentiostatic instrumentation) were performed under argon in dry and degassed CH_2Cl_2 at room temperature and at scan rates of 100, 250, and 500 mV/s. The electrolyte was 0.10 M Bu_4NPF_6. The working electrode was a platinum disk (1 mm in diameter), the counter electrode was a platinum wire, and the reference electrode was an Ag/AgCl electrode. For documentation, the potentials were corrected to the internal standard of Fc/Fc^+ in CH_2Cl_2 ($E_0^{0/+1}$ = 450 mV).[21]

Synthesis of Thioacetic Acid *S*-[4-(10-hexyl-10*H*-phenothiazin-3-ylethynyl)-phenyl] Ester (3a). 3-Ethynyl-10-hexyl-10*H*-phenothiazine (**1a**)[19c] (297 mg (0.97 mmol)) was placed in a 100-mL Schlenk flask under argon. Through a short column (diameter (Ø) = 1.5 cm, *L* = 3 cm) filled with dry, basic alumina (dried at 70 °C for 1 d in a dry oven and cooled under an atmosphere of argon) that was placed on top of the Schlenk flask; subsequently, 8 mL of dry *N*-ethyl diisopropyl amine and 8 mL of dry THF were filtered in the Schlenk flask. After degassing the light yellow solution with argon for 10 min, 257 mg (0.92 mmol) of 1-(*S*-acetylthio)-4-iodo benzene (**2**)[22] and 33 mg (0.03 mmol) of $Pd(PPh_3)_4$ were added and, with mixing, was heated for 3 days to 40 °C, using a oil bath). The solvents were removed in vacuo and the residue was triturated with diethyl ether and filtered. The solvents of the filtrate were removed in vacuo and the residue was chromatographed on silica gel (Ø = 2.5 cm, *L* = 25 cm) with diethyl ether/pentane (1:25) to give 291 mg (69%) of **3a** as a light orange oil. R_f (diethyl ether/pentane 1:25) = 0.45. MS (FAB+) *m*/*z* (%): 459 (19), 458 (46), 457 (M^+, 100), 330 (10). IR (KBr), *ν*: 3059 cm^{-1} (w), 2950 (ss), 2927 (ss), 2855 (s), 2202 (m), 1850 (w, br), 1712 (ss), 1589 (s), 1574 (s), 1501 (ss), 1468 (ss), 1397 (s), 1335 (s), 1296 (m), 1251 (s), 1195 (m), 1130 (m, sh), 1118 (s, br), 1015 (m), 949 (m), 882 (m), 827 (ss), 749 (ss), 621 (s). UV/vis (CH_2Cl_2), λ_{max} (*ε*): 242 nm (21400), 280 (33500), 304 (28000), 358 (15500). Anal. Calcd. for $C_{28}H_{27}NOS_2$ (457.6): C, 73.48; H, 5.95; N, 3.06; S, 14.01. Found: C, 73.41; H, 6.17; N, 2.97; S, 13.89.

Thioacetic Acid *S*-[4-(10,10′-dihexyl-10*H*,10′*H*-[3,3′]biphenothiazinyl-7-ylethynyl)-phenyl] Ester (3b). 3-Ethynyl-10,10′-dihexyl-10*H*,10′*H*-[3,3′]-biphenothiazinyl (**1b**)[19f] (162 mg (0.27 mmol)) was placed in a 100-mL Schlenk flask under argon. Through a short column (Ø = 1.5 cm, *L* = 3 cm) filled with dry, basic alumina (dried at

(14) (a) Oka, H. *J. Mater. Chem.* **2008**, *18*, 1927–1934. (b) Okamato, T.; Kuratsu, M.; Kozaki, M.; Hirotsu, K.; Ichimura, A.; Matsushita, T.; Okada, K. *Org. Lett.* **2004**, *6*, 3493–3496. (c) Sun, D.; Rosokha, S. V.; Kochi, J. K. *J. Am. Chem. Soc.* **2004**, *126*, 1388–1401. (d) Kochi, J. K.; Rathore, R.; Le Maguères, P. *J. Org. Chem.* **2000**, *65*, 6826–6836. (e) Nishinaga, T.; Inoue, R.; Matsuura, A.; Komatsu, K. *Org. Lett.* **2002**, *4*, 1435–1438. (f) Pan, D.; Philips, D. L. *J. Phys. Chem. A* **1999**, *103*, 4737–4743.

(15) (a) Sailer, M.; Franz, A. W.; Müller, T. J. J. *Chem.—Eur. J.* **2008**, *14*, 2602–2614. (b) Franz, A. W.; Popa, L. N.; Müller, T. J. J. *Tetrahedron Lett.* **2008**, *49*, 3300–3303. (c) Franz, A. W.; Popa, L. N.; Rominger, F.; Müller, T. J. J. *Org. Biomol. Chem.* **2009**, *7*, 469–475.

(16) Barkschat, C. S.; Guckenberger, R.; Müller, T. J. J. *Z. Naturforsch.* **2009**, *64b*, 707–718.

(17) McDowell, J. J. H. *Acta Crystallogr., Sect. B: Found. Crystallogr.* **1976**, *B32*, 5–10.

(18) Uchida, T.; Ito, M.; Kozawa, K. *Bull. Chem. Soc. Jpn.* **1983**, *56*, 577–582.

(19) (a) Müller, T. J. J. *Tetrahedron Lett.* **1999**, *40*, 6563–6566. (b) Krämer, C. S.; Zeitler, K.; Müller, T. J. J. *Org. Lett.* **2000**, *2*, 3723–3726. (c) Krämer, C. S.; Müller, T. J. J. *Eur. J. Org. Chem.* **2003**, 3534–3548. (d) Sailer, M.; Nonnenmacher, M.; Oeser, T.; Müller, T. J. J. *Eur. J. Org. Chem.* **2006**, 423–435. (e) Bucci, N.; Müller, T. J. J. *Tetrahedron Lett.* **2006**, *47*, 8323–8327. (f) Bucci, N.; Müller, T. J. J. *Tetrahedron Lett.* **2006**, *47*, 8329–8332. (g) Hauck, M.; Schönhaber, J.; Zucchero, A. J.; Hardcastle, K. I.; Müller, T. J. J.; Bunz, U. H. F. *J. Org. Chem.* **2007**, *72*, 6714–6725.

(20) Hesse, M.; , Meier, H.; , Zeeh, B. *Spektroskopische Methoden in der Organischen Chemie*; Georg Thieme Verlag: Stuttgart, New York, 1991; p 69.

(21) Zanello, P. In *Ferrocenes*; Togni, A., Hayashi, T., Eds.; VCH: Weinheim, New York, Basel, Cambridge, Tokyo, 1995, 317−430.

(22) Gryko, D. T.; Clausen, C.; Roth, K. M.; Dontha, N.; Bocian, D. F.; Kuhr, W. G.; Lindsey, J. S. *J. Org. Chem.* **2000**, *65*, 7345–7355.

70 °C for 1 d in a dry oven and cooled under an atmosphere of argon) that was placed on top of the Schlenk flask subsequently 10 mL of dry *N*-ethyl diisopropyl amine and 10 mL of dry THF were filtered in the Schlenk flask. After degassing the light yellow solution with argon for 10 min, 73 mg (0.26 mmol) of 1-(*S*-acetylthio)-4-iodo benzene (**2**)[22] and 16 mg (0.01 mmol) of $Pd(PPh_3)_4$ were added and, with mixing, was heated for 3 days to 40 °C in an oil bath). The solvents were removed in vacuo and the residue was chromatographed on silica gel (Ø = 2.5 cm, L = 25 cm) with diethyl ether/pentane (1:25) to give after trituration with pentane 86 mg (44%) of **3b** as a yellow resin. R_f (diethyl ether/pentane 1:25) = 0.43. MS (FAB+) m/z (%): 741 (14), 740 (34), 739 (68), 738 (M^+, 100), 737 (13), 654 (14), 653 (16). IR (KBr), ν: 2954 cm^{-1} (m), 2927 (m), 2855 (w), 2205 (w), 2066 (w), 2010 (w), 1750 (w), 1704 (s), 1688 (s, sh), 1628 (m), 1579 (w), 1562 (w), 1460 (ss), 1417 (w), 1398 (w), 1381 (w), 1335 (w), 1241 (m, br), 1193 (w), 1119 (w, br), 808 (w), 748 (w). UV/vis (CH_2Cl_2), λ_{max} (ε): 236 nm (38900), 260 (42500, sh), 290 (69100), 308 (49900, sh), 376 (27100). HRMS calcd. for $C_{46}H_{46}N_2OS_3$: 738.2772; Found: 738.2764. Anal. Calcd. for $C_{46}H_{46}N_2OS_3$ (739.0): C, 74.76; H, 6.27; N, 3.79; S, 13.01; Found: C, 74.58; H, 6.19; N, 3.85; S, 13.10.

Thioacetic Acid *S*-{4-[7-(4-acetylsulfanylphenylethynyl)-10-methyl-10*H*-phenothiazin-3-ylethynyl]-phenyl} Ester (5a) and Thioacetic Acid *S*-[4-(7-ethynyl-10-methyl-10*H*-phenothiazin-3-ylethynyl)-phenyl] Ester (5b). 3,7-Diethynyl-10-methyl-10*H*-phenothiazine (**4a**)[19c] (147 mg (0.56 mmol)) and 39 mg (0.03 mmol) of $Pd(PPh_3)_4$ were placed in a 50-mL Schlenk flask under argon. Through a short column (Ø = 1.5 cm, L = 3 cm) filled with dry, basic alumina (dried at 70 °C for 1 d in a dry oven and cooled under an atmosphere of argon) that was placed on top of the Schlenk flask subsequently 10 mL of dry *N*-ethyl diisopropyl amine and 10 mL of dry THF were filtered in the Schlenk flask. After degassing the light yellow solution with argon for 10 min, 300 mg (1.08 mmol) of 1-(*S*-acetylthio)-4-iodo benzene (**2**)[22] was mixed and heated for 2 days to 40 °C in an oil bath. The solvents were removed in vacuo and the residue was triturated with THF and filtered. The solvents of the filtrate were removed in vacuo, and the residue was chromatographed on silica gel (Ø = 2.5 cm, L = 25 cm) with dichloromethane/hexane (1:20) and gradually increasing the amount of dichloromethane to give 26 mg (11%) of **5a** as a dark yellow solid and 152 mg (0.27 mmol = 50%) of **5b** as a dark yellow powder.

5a: MP = 150−151 °C. R_f (dichloromethane/hexane ratio = 1:20) = 0.22. MS (EI+, 70 eV) m/z (%): 412 (29), 411 (M^+, 100), 370 (10), 369 (33), 368 (19), 355 (10), 354 (35), 353 (22). IR (KBr), ν: 3279 cm^{-1} (m, sh), 2900 (w), 2200 (w), 2100 (w), 1694 (m), 1628 (w), 1579 (w), 1504 (w), 1469 (ss), 1393 (m), 1336 (s), 1269 (m), 1154 (w), 1128 (m), 1090 (w), 1016 (w), 955 (w), 824 (s). UV/vis (CH_2Cl_2), λ_{max} (ε): 248 (20000), 282 (44900), 306 (29300), 362 (7300), 358 (15500). HRMS calcd. for $C_{25}H_{17}NOS_2$: 411.0751; Found: 411.0758 (MS).

5b: Mp. 224−225 °C. MS (EI+, 70 eV) m/z (%): 563 (25), 562 (39), 561 (M^+, 100), 521 (21), 520 (35), 519 (89), 518 (23), 478 (15), 477 (36), 476 (24), 463 (18), 462 (43), 461 (40), 460 (11). IR (KBr), ν: 2200 cm^{-1} (w), 1700 (s), 1639 (ss, br), 1543 (s), 1490 (ss), 1393 (w), 1337 (s), 1269 (w), 1155 (m), 1127 (m), 1015 (w), 954 (w), 882 (w), 826 (m). UV/vis (CH_2Cl_2), λ_{max} (ε): 290 (55400, sh), 306 (61600), 380 (21400). Anal. Calcd. for $C_{33}H_{23}NO_2S_3$ (561.7): C, 70.56; H, 4.13; N, 2.49; S, 17.12. Found: C, 70.45; H, 4.19; N, 2.53; S, 16.85.

Thioacetic Acid *S*-{4-[7″-(4-acetylsulfanylphenylethynyl)-10,10′,10″-trihexyl-10*H*,10′*H*,10″*H*-[3,3′,7′,3″]terphenothiazin-7-ylethyynyl]-phenyl} Ester (5c). 7,7″-Diethynyl-10,10′,10″-trihexyl-10*H*,10′*H*,10″*H*-[3,3′,7′,3″]-terphenothiazine (**4b**)[19c] (279 mg (0.31 mmol)) was placed in a 50-mL Schlenk flask under argon. Through a short column (Ø = 1.5 cm, L = 3 cm) filled with dry, basic alumina (dried at 70 °C for 1 d in a dry oven and cooled under an atmosphere of argon) that was placed on top of the Schlenk flask subsequently 10 mL of dry *N*-ethyl diisopropyl amine and 10 mL of dry THF were filtered in the Schlenk flask. After degassing the light yellow solution with argon for 10 min 174 mg (0.62 mmol) of 1-(*S*-acetylthio)-4-iodo benzene (**2**)[22] and 29 mg (0.02 mmol) of $Pd(PPh_3)_4$ and, with mixing, was heated for 5 days to 40 °C in an oil bath). The solvents were removed in vacuo, and the residue was chromatographed on silica gel (Ø = 4 cm, L = 20 cm) with dichloromethane/pentane (1:3) and gradually increasing the amount of dichloromethane to give after trituration with pentane 105 mg (28%) of **5c** as a yellow powder. Mp. 118−122 °C. R_f (dichloromethane/pentane 1:4) = 0.34. MS (FAB+) m/z (%): 1197 (16), 1196 (35), 1195 (66), 1194 (95), 1193 (M^+, 100), 1192 (17), 1152 (10), 1151 (14), 1151 (9), 1122 (9), 441 (13), 419 (16). IR (KBr), ν: 2954 cm^{-1} (m, br), 2926 (m), 2855 (w), 2199 (w, br), 1710 (s), 1624 (w), 1581 (w), 1460 (ss), 1377 (m), 1355 (m), 1242 (s), 1191 (m), 1153 (m), 1108 (m), 1015 (w), 948 (w), 876 (w), 820 (s), 808 (s), 732 (w). UV/vis (CH_2Cl_2), λ_{max} (ε): 238 (59700, sh), 292 (132700), 384 (53900). Anal. Calcd. for $C_{74}H_{71}N_3O_2S_5$ (1194.7): C, 74.39; H, 5.99; N, 3.52; S, 13.42; Found: C,74.59; H, 6.05; N, 3.68; S, 13.28.

Preparation of Sample Films of 3a, 5a, and 5b on Gold. A freshly prepared 0.1 mM solution of either **3a**, **5a**, or **5b** (10 mL) in THF was degassed with argon for 10 min using a long thin syringe needle. A piece of a gold-coated silicon wafer (Au thickness of 100 nm, 5 nm of titanium as a adhesion promoter, obtained from Georg Albert Beschichtungen, Heidelberg, Germany) ~20 mm × 20 mm in size and 0.4 mL of a 0.1 M aqueous solution of NH_4OH then were added. Degassing with argon was continued for 10 min to ensure a thorough mixing of the aqueous solution and the organic solvent. The substrate was left in solution under argon for different exposure times (10 min, 30 min, 60 min (1 h), 300 min (5 h), 1440 min (24 h), 7200 min (120 h)). The wafer piece then was taken out of the solution and rinsed with THF and ethanol in an ultrasonic bath. Finally, the substrate bearing an ultrathin film of one of the compounds **3a**, **5a**, or **5b** was dried in a constant stream of dry nitrogen and stored under an inert gas atmosphere until further analysis.

Surface Characterization. *Ellipsometry*. Spectral ellipsometry was performed ex situ, using a J. A. Woollam M-44 spectral ellipsometer. For calibration (i.e., the determination of the incident angle), thermally oxidized SiO_2/Si wafers were utilized. The optical constants of the thin gold layer were obtained from measurements on freshly evaporated uncoated samples. For data analysis, a three-layer model (air/organic layer/gold) was applied, whereby the optical properties of the organic layer were described by a Cauchy model, assuming a refractive index of 1.490 at 500 nm, which had given good agreement with XPS results in a prior study on aromatic SAMs.[23]

Contact Angle Measurements. Advancing contact angles were measured with a Krüss G1 goniometer, using purified deionized water (Milli-Q plus system, Millipore, Eschborn, Germany).

Infrared Spectroscopy (*IRRAS*). Infrared spectra were taken with a dry-air purged Bio-Rad spectrometer (model FTS 175c) that was equipped with a liquid-nitrogen-cooled MCT detector, an aluminum wire-grid polarizer, and a multiangle reflection unit set to an incidence angle of 75°. All spectra were normalized to the spectrum of a gold substrate coated with a perdeuterated SAM (octadecanethiol-d_{37}) acquired under the same conditions.

(23) Stoycheva, S.; Himmelhaus, M.; Fick, J.; Korniakov, A.; Grunze, M.; Ulman, A. *Langmuir* **2006**, *22*, 4170–4178.

Scheme 1. Synthesis of Phenylethynyl (Oligo)Phenothiazinyl Thioacetates 3 and 5

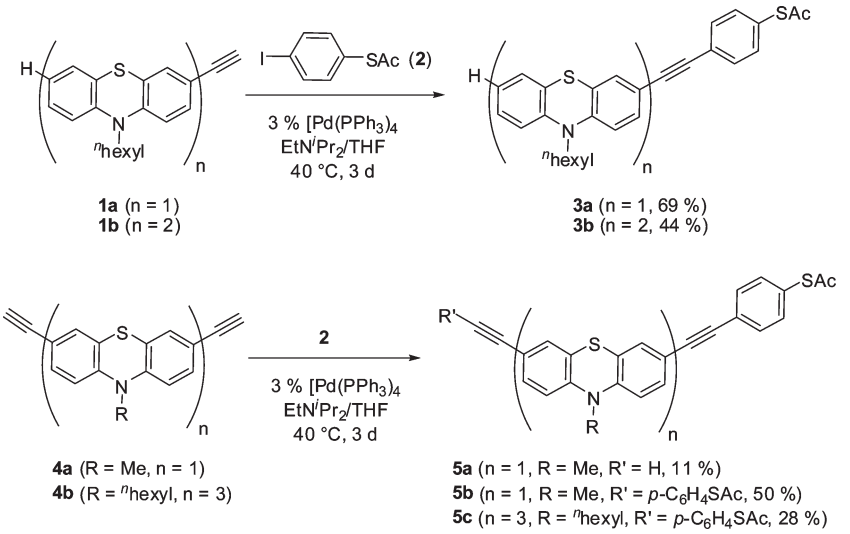

Table 1. Absorption[a] and Selected Emission Data[b] of (Oligo)Phenothiazinyl Thioacetates 3 and 5

compound	absorption $\lambda_{max,abs}$ [nm]	emission $\lambda_{max,em}$ [nm] (Φ_f)	Stokes shift, $\Delta\tilde{\nu}$ [cm^{-1}]
3a	242, 280, 304, 358		
3b	236, 260, 290, 308, **376**	**491** (0.51)	6200
5a	248, 282, 306, 362, 358		
5b	290, 306, 380		
5c	238, 292, **384**	**490** (0.41)	5600

[a] Recorded in CH_2Cl_2. [b] Recorded in $CHCl_3$ with perylene as a standard.

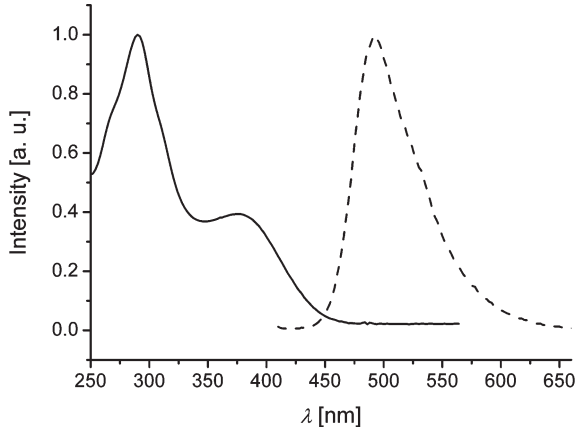

Figure 1. Normalized absorption (solid line) and emission (dashed line) spectra of thioacetate **3b** (recorded in dichloromethane, $T = 298$ K).

X-ray Photoelectron Spectroscopy (*XPS*). X-ray photoelectron spectroscopy was performed with a Leybold Max 200 spectrometer applying an Al Kα X-ray source operated at 200 W and a spherical sector-type analyzer. Survey spectra were acquired at a constant pass energy of 96 eV, detail scans at 48 eV. The binding energy scale was referenced to the Au $4f_{7/2}$ peak at 84.0 eV. For details of the spectra evaluation, we refer to the literature.[23]

Results and Discussion

Synthesis and Electronic Properties of the Phenylethynyl Phenothiazinyl Thioacetates. The synthesis of alkynylated phenothiazines by Sonogashira coupling was previously established in our laboratories,[19a,c,f] and its application to terminal phenothiazinyl alkynes **1** and diynes **4** with 1-(*S*-acetylthio)-4-iodo benzene (**2**)[22] causes the formation of phenylethynyl (oligo)phenothiazinyl thioacetates **3** and **5** in moderate to good yields (see Scheme 1). The structures of the thioacetates **3** and **5** are unambiguously supported by ^{1}H and ^{13}C NMR, and IR spectroscopy, as well as mass spectrometry and correct combustion analysis. The electronic properties of the phenylethynyl phenothiazinyl thioacetates **3** and **5** have been investigated by optical spectroscopy (see Table 1). UV/vis and selected fluorescence

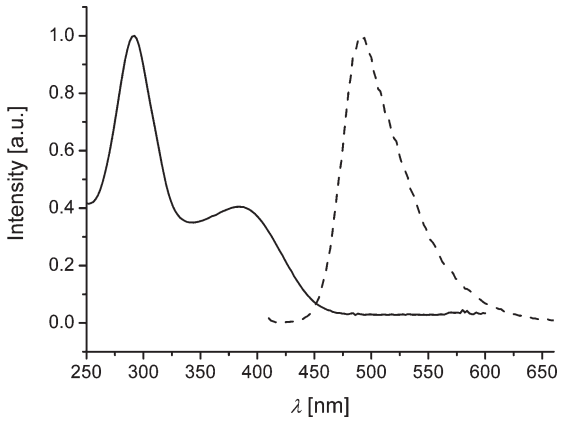

Figure 2. Normalized absorption (solid line) and emission (dashed line) spectra of thioacetate **5c** (recorded in dichloromethane, $T = 298$ K).

Table 2. Oxidation Potentials of Thioacetates 3 and after Chemisorption of Their In Situ Generated Thiols on the Gold Electrodes[a]

	Thioacetates[b]		Thiols after Chemisorption[c]			
compound	$E_{1/2}^{0/+1}$ [mV]	$E_{1/2}^{+1/+2}$ [mV]	$E_{1/2}^{0/+1}$ [mV]	E_{pa}^{1} [mV]	E_{pa}^{2} [mV]	E_{pc}^{1} [mV]
3a[d]	781		617[f]			
3b[e]	437	599	562[g]	765	865	739

[a] Solvent, $T = 20$ °C, $v = 100$ mV/s, electrolyte: ^{n}Bu$_4$N$^+$PF$_6^-$, Au working electrode, Pt counter electrode, Ag/AgCl reference electrode. [b] Normalized to the internal standard Fc/Fc$^+$ in CH_2Cl_2 ($E_0^{0/+1} = 450$ mV).[21] [c] Without normalization to Fc/Fc$^+$. [d] Recorded in THF. [e] Recorded in CH_2Cl_2. [f] $\Delta E_{pa} - E_{pc} = 34$ mV. [g] $\Delta E_{pa} - E_{pc} = 17$ mV.

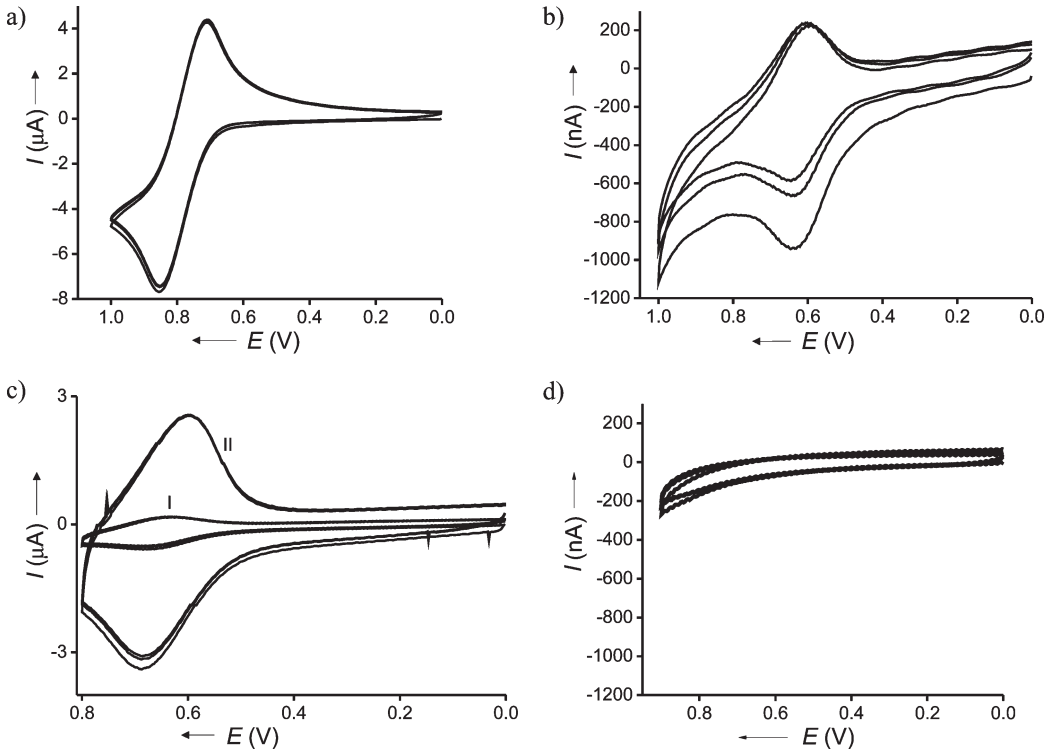

Figure 3. (a) Cyclic voltammogram of thioacetate **3a** in THF at $v = 100$ mV/s (platinum electrode). (b) Cyclic voltammogram after chemisorption of the in-situ-formed thiols (prepared from c_0(**3a**) = 10^{-3} mol/L in THF by adding 3 mL of 0.1 M aqueous ammonium hydroxide solution in the presence of a Au electrode and leaving the electrode in the solution for 30 min; the modified electrode then was rinsed with CH_2Cl_2, water, and THF) on a gold electrode at $v = 100$ mV/s. (c) Modified electrode at $v = 100$ mV/s (curve I) and $v = 1000$ mV/s (curve II) (gold electrode). (d) Cyclic voltammogram of the electrolyte solution depicted in panels (a)−(c) after exchange of the **3a** modified electrode against a platinum working electrode.

spectra reveal that absorbance occurs at the edge to the UV edge to the visible and oligophenothiazines **3b** and **5c** display considerable greenish-blue luminescence with 51% and 41% fluorescence quantum yield and large Stokes shifts ($\Delta\tilde{v}$ = 5600−6200 cm^{-1}) (see Figures 1 and 2).

As previously demonstrated for amine-terminated conjugated molecular wires,[24] the chemisorption of the phenothiazines **3** was first probed by semiquantitative cyclovoltammetric studies in the anodic region (scan area up to 1.0 V). Chemisorption experiments on a gold electrode were directly carried out from argon degassed THF solutions of the thioacetates of **3** by immersing the gold electrode. Then, by in situ deprotection of the thioacetates with aqueous ammonia, the liberated thiol functionalities were reacted with the electrode surface for 30 min. After rinsing the electrode with dichloromethane, water, and THF, the prepared electrodes were plunged into the electrolyte solution of the cyclic voltammetry cell and the cyclic voltammograms were recorded (see Table 2, as well as Figures 3 and 4).

Thus, in multisweep experiments with a platinum working electrode, the oxidations of acetates **3** to the monocations and dications are fully reversible, in accordance with Nernstian behavior (see Figures 3a and 4a). All multisweep experiments (three cycles) were conducted with an initial potential of 0 V and reversal potentials of 0.9−1.0 V. For acetate **3b**, expectedly, two distinctly separated, reversible oxidations can be found, because of unsymmetrical substitution of the dyad. After deprotection and chemisorption of the thiols on gold electrodes, the reversibility of the first oxidations is maintained showing the expected narrow differences of anodic and cathodic peak potentials in the slightly distorted bell-shaped cyclic voltammograms characteristic for electrode-adsorbed redox-active molecules with Nernstian behavior (see Figures 3b and 4b). This is also supported by the linear correlation between peak currents and scan rate (see Figure 3c).[25] Upon increasing the scan rate from 100 mV/s to 1000 mV/s, an approximate 10-fold increase of anodic and cathodic peak currents can be detected. The gradual depression of the oxidative current peak potentials (Figures 3b and 4b) converges to constant values that are then maintained over multiple sweeps and also at two different scan rates (see Figure 3c). Hence, electropolymerization of the chemisorbed species to conjugated polymers can be excluded. Since perfect orientation of the thiol substrates on the gold electrode surface cannot be expected upon chemisorption, it appears that multiple redox cycles, leading to constant peak currents, indicate a post-chemisorption self-organization on the electrode surface.

After the multisweep experiments, the electrolyte solutions were checked for eventually desorbed molecules. The modified Au electrodes were replaced by a platinum

(24) Lambert, C.; Kriegisch, V. *Langmuir* **2006**, *22*, 8807–8812.

(25) Bard, A. J.; Faulkner, L. R. In *Electrochemical Methods—Fundamentals and Applications*, 2nd Edition; John Wiley and Sons: New York, Chichester, Weinheim, Brisbane, Singapore, Toronto, 2001; Chapter 14.3, p 589.

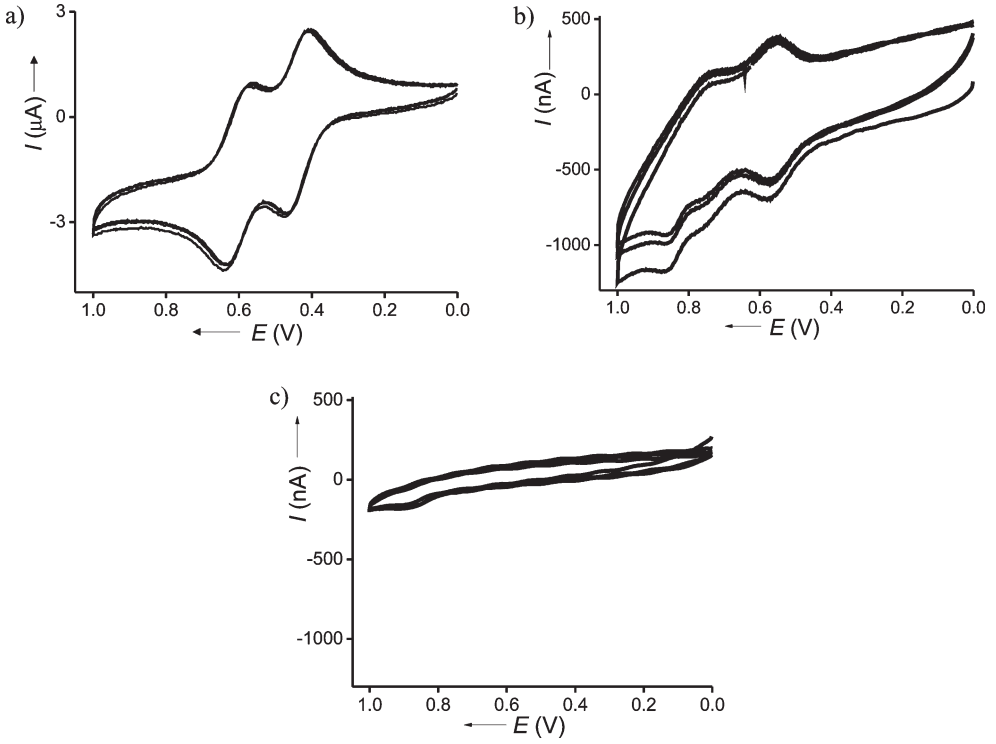

Figure 4. (a) Cyclic voltammogram of thioacetate **3b** in CH_2Cl_2 at $v = 100$ mV/s (platinum electrode). (b) Cyclic voltammogram after chemisorption of the in-situ-formed thiols (prepared from c_0(**3b**) = 10^{-3} mol/L in THF by adding 3 mL of 0.1 M aqueous ammonium hydroxide solution in the presence of an Au electrode and leaving the electrode in the solution for 30 min; the modified electrode then was rinsed with CH_2Cl_2, water, and THF) on an Au electrode at $v = 100$ mV/s. (c) Cyclic voltammogram of the electrolyte solution depicted in panels (a)−(c) after exchange of the **3b** modified electrode against a platinum working electrode.

Table 3. Layer Thickness by Ellipsometry (Å) and Contact Angle (°) for Ultrathin Layers of Compounds 3a, 5a, and 5b on Gold for Various Incubation Times

	3a		5a		5b	
incubation time [min]	thickness [Å]	contact angle [°]	thickness [Å]	contact angle [°]	thickness [Å]	contact angle [°]
10	12.7	79	11.9	74	18.5	69
30	12.2	87	11.9	74	18.2	77
60 (1 h)	15.2	84	14.6	76	20.8	76
300 (5 h)	15.4	90	17.8	75	23.5	76
1440 (24 h)	13.6	88	18.3	73	24.3	74
7200 (120 h)	15.6	89	19.2	73	27.1	75

working electrode and cyclic voltammetry of the electrolyte solutions was performed (see Figures 3d and 4c), indicating that, within the applied voltage range and after multiple oxidation and reduction cycles (see Figures 3b, 3c, and 4b), neither leaching from the electrode nor degradation of the chemisorbed species can be found. In contrast to pyrroles and thiophenes, phenothiazines are quite stable, under the conditions of one-electron oxidations,[15] even if they are chemisorbed, as in the presented cases. Therefore, (oligo)phenothiazines chemisorbed via thiol ligation should be stable enough and should behave favorably for the formation of ultrathin films of self-assembled monolayers.

Preparation and Investigation of Sample Films of 3a, 5a, and 5b on Gold. For preparing ultrathin films by self-assembly, the thioacetates **3a**, **5a**, and **5b** were subjected to chemisorption experiments with suitable gold-coated silicon wafers to gain insight into the extent to which these complex molecules are able to form ordered and dense SAMs, which is a prerequisite for their practical application in molecular electronics. The experiments were performed

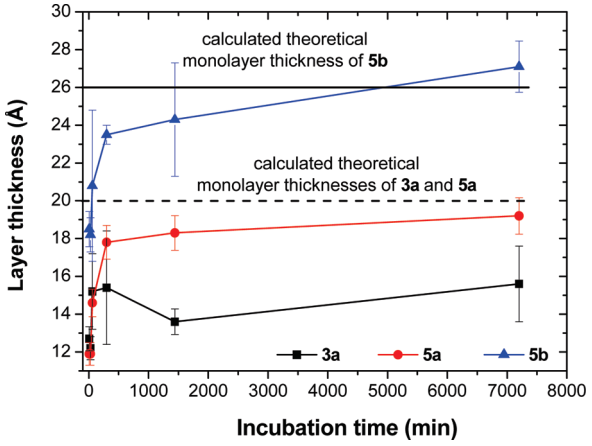

Figure 5. Layer thicknesses of the films of compounds **3a**, **5a**, and **5b** on gold determined by ellipsometry, compared to calculated monolayer thicknesses of **3a** and **5a** (dashed line) and **5b** (solid line).

in the presence of aqueous ammonium hydroxide solution to promote the base-mediated saponification of the thioacetates, thus leading to the in situ liberation of thiols

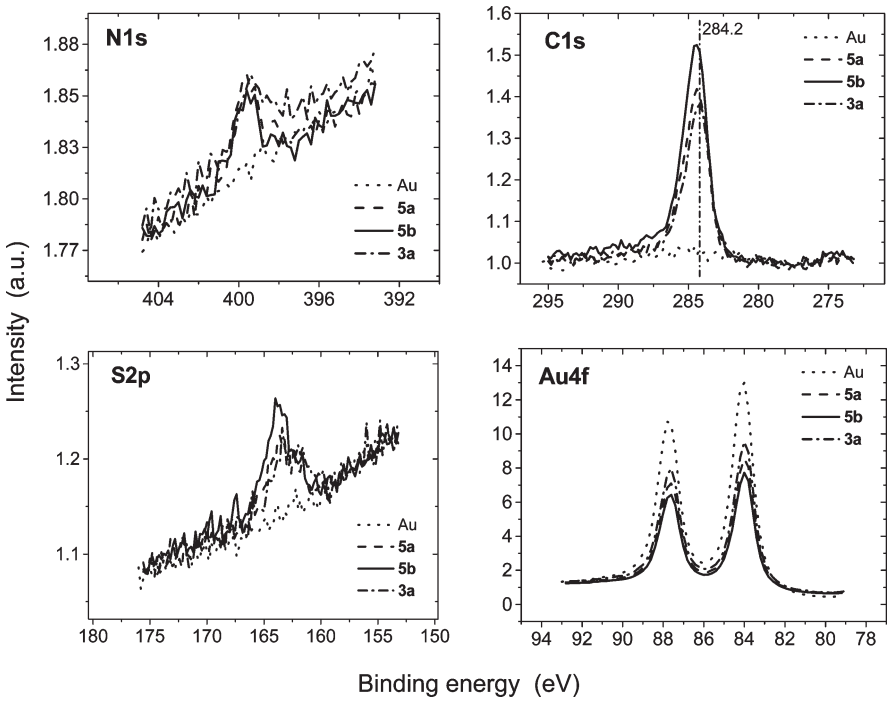

Figure 6. Detail spectra of N 1s, C 1s, S 2p, and Au 4f of samples **3a**, **5a**, and **5b** on gold.

Table 4. Peak Positions of the Detail Spectra of Samples 3a, 5a, and 5b on Gold

compound	N 1s	C 1s	S $2p_{3/2}$	Au $4f_{7/2}$
3a	399.3	284.2	162.5	84.0
5a	399.6	284.2	163.1	84.0
5b	399.6	284.3	163.4	84.0

Table 5. Calculated Layer Thicknesses (by Attenuation of the Gold Signal) and Stoichiometric Ratios C 1s/N 1s und C 1s/S 2p of Samples 3a, 5a, and 5b on Gold Determined by the Statistic and Layer Models

		C 1s/S 2p		C 1s/N 1s	
compound	layer thickness by XPS [Å][a]	statistic model[a]	layer model	statistic model[a]	layer model
3a	13.5 (20)	13.3 (13)	9.3	18.5 (26)	20
5a	16.9 (20)	19 (11.5)	12.6	17.9 (23)	16
5b	20.8 (26)	12.6 (9.3)	9	32 (29)	26.6

[a] Calculated theoretical values are given in parentheses.

that can undergo the self-assembly on a gold surface. This strategy allows the triggering of the chemisorptions process and, thus, the SAM formation, which is another interesting aspect of the systems of the present study, in view of the formation of complex molecular electronics structures.

Kinetic Measurements. Ultrathin layers of compounds **3a**, **5a**, or **5b** on gold were prepared with various incubation times (10 min, 30 min, 60 min, 300 min, 1440 min, 7200 min) in a 0.1 mM THF solution. An estimation of the film formation kinetics was then obtained by immediately measuring the thickness of layers and their contact angle (see Table 3) after removal of the samples from the incubation solution and subsequent rinsing, as detailed in the Experimental Section.

According to force field calculations, the intramolecular distances between the thiol S atoms and the distal-ring C atoms in compounds **3a** and **5a** are ~16 Å. Upon adding the Au−S bond length of 2 Å, the bond length of the ethynyl moiety (1.2 Å), and the extension of the hexyl side chain (1.5 Å),[26] a monolayer of orthogonally arranged molecules should be ~20 Å thick. For compound **5b**, the intramolecular distance between both terminal thiol S atoms calculates to 22 Å, and addition of the Au−S and S−H bonds yields a calculated layer thickness of 26 Å, also assuming an orthogonal orientation of the molecules on the surface.

Ellipsometry (shown in Figure 5) indicates that all representatives relatively quickly (300 min) form complete films, which only slightly have a tendency to reorganize with time (7200 min). The films of compound **5a** and **5b** correspond to the calculated theoretical monolayer thicknesses with orthogonal orientation of the molecules in good accordance. However, films of the *N*-hexyl-substituted derivative **3a** reveal a deviation by almost 5 Å. Presumably, the hexyl side chains hamper a close packing within the layer. According to these results, all three molecules give rise to monolayer formation without competing multilayer generation.

The water contact angle of the samples almost remains constant over time. With angles of 71° (**5b**) and 73° (**5a**), good accordance with the literature data for aromatic SAMs on gold is obtained.[27] Sample **3a** furnishes an angle

(26) Ulman, A. In *An Introduction to Ultrathin Organic Films*; Academic Press: Boston, 1991.

(27) (a) de Boer, B.; Meng, H.; Perepichka, D. F.; Zheng, J.; Frank, M. M.; Chabal, Y. J.; (b) Bao, Zh. *Langmuir* **2003**, *19*, 4272–4284. (c) Tai, Y.; Shaporenko, A.; Rong, H.-T.; Buck, M.; Eck, W.; Grunze, M.; Zharnikov, M. *J. Phys. Chem. B* **2004**, *108*, 16806–16810. (d) Kang, J. F.; Ulman, A.; Liao, S.; Jordan, R. *Langmuir* **2001**, *17*, 95–106.

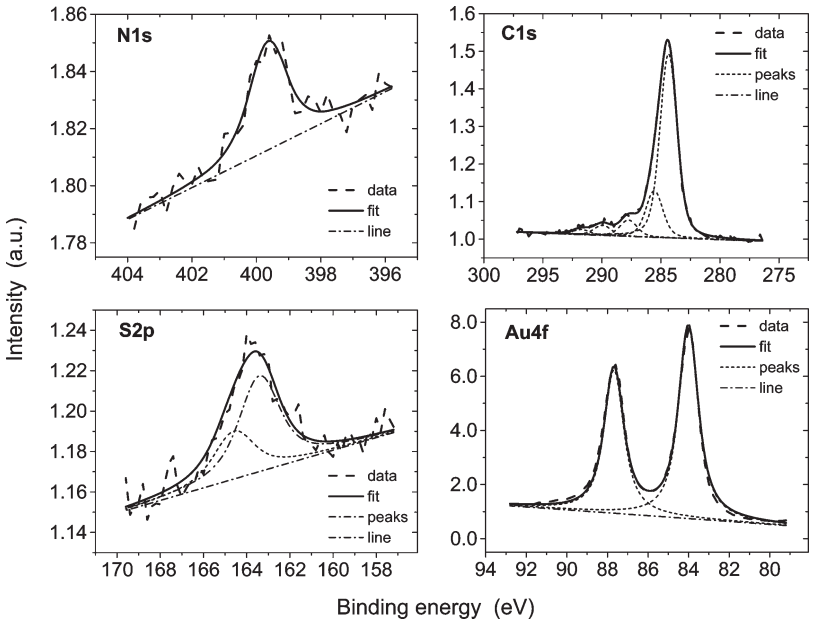

Figure 7. Detail spectra of N 1s, C 1s, S 2p, and Au 4f of sample **5b** on gold with the Voigt fit functions.

of 90° that can be rationalized by the hydrophobic character and influence of the *N*-hexyl side chain.

Further information on coverage and chemical composition of the films was obtained by XPS of the samples with incubation times of 7200 min. Expectedly, carbon, sulfur, and nitrogen were detected, as shown by the detail spectra (see Figure 6) and the corresponding peak positions (shown in Table 4). The bond energies were normalized to the Au $4f_{7/2}$ peak at 84.0 eV. The absence of oxygen indicates the successful deprotection of the thioester. The peak positions of all three molecules are almost identical, because of their similar chemical structure and, thus, similar chemical shift of the respective moieties. The S 2p peaks at 163 eV indicate thiolate formation.[28]

The Au 4f and C 1s intensities are indicative for decreasing layer thicknesses from **5b** over **5a** to 3a. The exact layer thicknesses were determined from the attenuation of the Au signal ($\lambda = 35$), which is due to the organic overlayer, using both a statistic and a layer model for calculation of the stoichiometric ratios of C 1s/S 2p and C 1s/N 1s (see Table 5). In the statistic model, an irregular distribution of the molecules within the layer is assumed, which is synonymous with an arbitrary height distribution of the individual atoms comprising the molecules within the film. Therefore, on average, all different types of atoms within the molecule experience the same attenuation of their photoemission. In contrast, the layer model assumes a defined alignment and orientation of the molecules, resulting in a well-defined height profile of the film and, thus, different attenuation for atoms located in different height levels. Therefore, based on the agreement of the predictions made by these two models, e.g., in terms of calculated stoichiometric ratios, evidence on the molecular structure of the film may be obtained. For such quantification, the different emission peaks were fitted to Voigt profiles. Since the spectra of all three molecules turned out to be very similar, only the evaluated detail spectra of sample **5b** are depicted in Figure 7, including their respective Voigt fits, as an example. As previously reported for mercapto biphenyl spectra, satisfactory fitting of the C 1s peak could be achieved only when five individual Voigt profiles with different positions were assumed, because of its asymmetry at the higher-binding-energy side.

The causes for this asymmetry are related to the structure of the main emission peak, which is broadened by various chemical shifts, the varying attenuation of the photoemission of the different C atoms, according to their position within the layer, and the appearance of so-called "shakeup signals" within the aromatic matrix.[29] The layer thicknesses determined by this method yield slightly smaller values, in comparison to the theoretically calculated thicknesses and those determined by ellipsometry. This deviation could have its origin in the uncertainty in determining the ellipsometry refractive indices and/or the error in the mean free path length (λ) used in XPS analysis.[23] Despite these minor differences, the stoichiometric C 1s/S 2p ratios of samples **5a** and **5b** determined by the layer model fit very nicely with the theoretically calculated values (see Table 5). The deviation is larger if the statistic model is used. This better agreement with the layer model indicates a well-ordered and oriented alignment of the molecules. In contrast, for sample **3a**, the statistic model has obviously better applicability, thus indicating an irregular distribution of the molecules within the film.

For the C 1s/N 1s ratios, the best-fitting results were obtained for sample **5b**. However, note that, because of the low intensities of the S 2p and N 1s signals leading to inaccuracies upon fitting, a significant error is made for

(28) Himmelhaus, M.; Gauss, I.; Buck, M.; Eisert, F.; Wöll, C.; Grunze, M. *J. Electron Spectrosc. Relat. Phenom.* **1998**, *92*, 139–149.

(29) Shaporenko, A.; Heister, K.; Ulman, A; Grunze, M.; Zharnikov, M. *J. Phys. Chem. B* **2005**, *109*, 4096–4103.

the calculation of these stoichiometric ratios. Therefore, these data should rather be considered as a qualitative affirmation of the film formation than a precise way to determine the exact packing density of the molecules. According to ellipsometry, contact angle, and XPS data, all three molecules form monolayers on gold relatively quickly (within 300 min (or 5 h)). Still, after 7200 min (120 h), sample **3a** has a lower layer thickness, indicating a lower degree of coverage. The undefined nature of the layer is also supported by the C 1s/S 2p ratio and could be caused by the disturbing effect of the hexyl side chain.

The aforementioned results indicate the formation of well-ordered monolayers, in particular, for the moieties **5a** and **5b**, the structure of which thus may be further analyzed by IRRAS to obtain insight into the average molecular orientation. This can be achieved by taking advantage of the dipole selection rule for IR spectroscopy on metal surfaces, which states that an IR-allowed resonance is only observable in IRRAS if it is not oriented parallel to the metal surface. Accordingly, depending on the appearance or disappearance of characteristic group resonances, the average orientation of the adsorbed molecules can be assessed.

Figure 8 displays IRRA spectra of SAMs of **3a**, **5a**, and **5b**, prepared on gold wafer pieces and immersed into the respective solution for 120 h. In Figures 8a and 8b, the characteristic resonances of the terminal alkynyl group of **5a** are shown, which indicate—because of their mere presence—that the molecules in the film formed by **5a** are oriented toward the surface normal. This observation, which is in agreement with the results obtained by ellipsometry and XPS, is further corroborated by the fingerprint spectra of the SAMs, as shown in Figure 6c. Except for the highest and lowest modes, indicated at 1577 and 821 cm^{-1}, respectively, all other observable peaks can be attributed to molecular resonances with an orientation of their transition dipole moments parallel to the molecular main axis (for mode assignments, see Table S1 in the Supporting Information). This actually validates that the molecular main axis of the molecules must have an orientation very close to the surface normal, which further suggests a high packing density within the monolayer. In fact, the sharpness of the peaks and the band intensity of the features observable in the spectrum of **5a** indicates that this film is comprised of the highest degree of order of all three molecules studied, and, therefore, also the highest molecular density. Otherwise, i.e., in terms of resonant features, the spectra obtained from **5a** and **5b** look basically the same. The spectrum of **3a** shows fewer features, because of the higher symmetry of its phenothiazine system, which increases the number of IR-forbidden vibrational modes. The lower intensity observed here is consistent with a lower degree of order, which increases the average tilt angle and, thus, increases the not-observable contribution of the transition dipole moments in a direction parallel to the surface.

Altogether, the IR spectra are in good agreement with the results of ellipsometry and XPS, in that, particularly, the SAMs of **5a** and **5b** are well-ordered, with an orientation

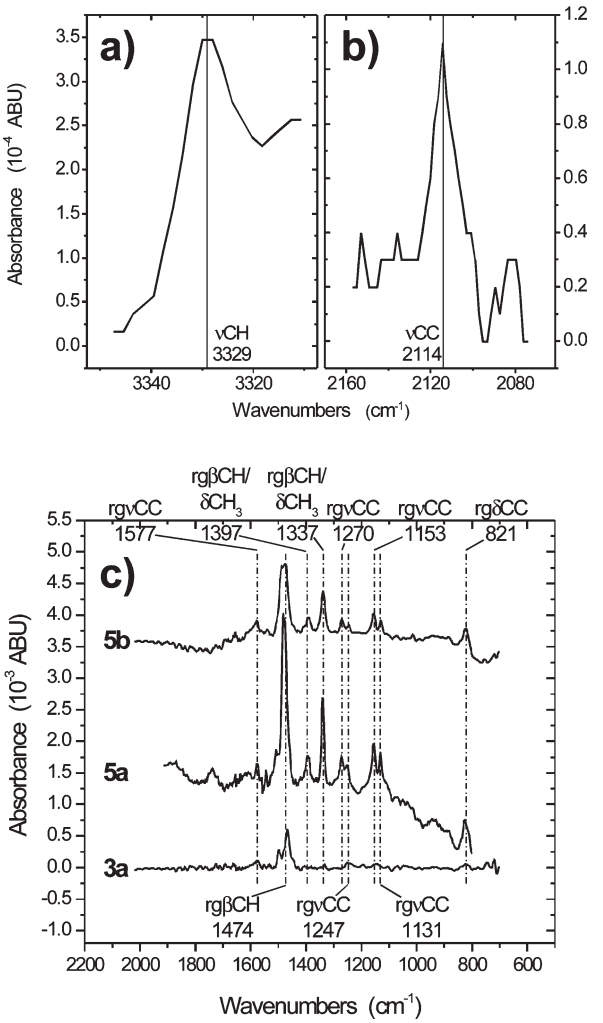

Figure 8. Reflection absorption infrared spectra of SAMs of **3a**, **5a**, and **5b**, respectively, on gold wafer pieces after 120 h of immersion into the respective solution: (a) terminal alkynyl CH valence vibration of a SAM formed by **5a**; (b) terminal alkynyl CC valence vibration of the SAM shown in panel (a); (c) region of the CH stretching vibrations. The spectra in panel (c) are vertically displaced for clarity; the indicated mode positions were averaged over those obtained from all three molecules. For the individual mode positions, as well as further details, we refer to the Supporting Information. Abbreviations: rg = ring, ν = stretching, β = bending, δ = deformation, s = symmetric, as = asymmetric.

of the molecular main axis close to the surface normal. For a more-detailed analysis of the IRRAS data, including the study of the film formation kinetics, we refer to the Supporting Information.

Investigation of the Density of Sample Films. The aforementioned surface analysis clearly shows that **5a**, **5b**, and **3a** form self-assembled monolayers on gold, which are—particularly for **5a** and **5b**—well-ordered, given the structural complexity of the molecules. In particular, it can be excluded that the molecules form multilayers. However, the density of the packing that is achieved has not yet become clear, i.e. whether it corresponds to full coverage, where each surface site is occupied by a molecule, or whether film formation levels off at lower coverage. In particular, for the proposed application as molecular switches, this is an important question, because any unoccupied surface site might lead to electrical bypasses in a later application.

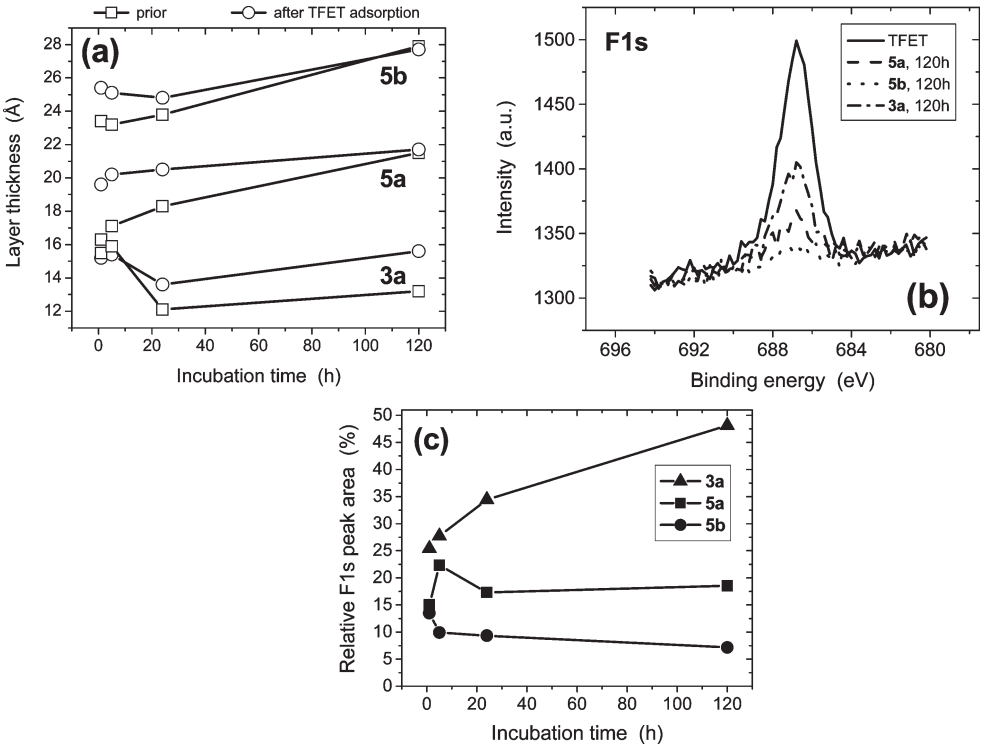

Figure 9. (a) Change of the layer thicknesses of samples **3a**, **5a**, and **5b** with increasing incubation time prior to and after the post-adsorption of trifluoroethane thiol. (b) F 1s signal in the XPS spectra of samples **3a**, **5a**, and **5b** after the adsorption of trifluoroethane thiol. (c) Relative peak area of the F 1s peaks of samples of **3a**, **5a**, and **5b** normalized to that of a TFET SAM on gold, in dependence of the incubation time in the respective phenothiazine derivative solution. The TFET post-adsorption time was kept fixed at 24 h.

Therefore, the density of the SAMs of **3a**, **5a**, and **5b** was determined by performing post-adsorption experiments with trifluoroethane thiol (TFET). TFET was chosen because the molecule is small and, thus, may diffuse easily into the phenothiazine film and, furthermore, can be easily detected and quantified via XPS, because of its fluorine moieties. Thus, after preparation of SAMs of **3a**, **5a**, and **5b** on gold as previously described (1−120 h of incubation), the samples were placed into a 1 mM solution of TFET in ethanol for 24 h. After rinsing with ethanol, the samples then were investigated by ellipsometry, contact angle, and XPS measurements.

The layer thicknesses of samples **5a** and **5b** at shorter incubation times are slightly increased after post-adsorption of TFET (Figure 9a), indicating that the native films still had defects. This causes an increase of the average layer thickness, as revealed by ellipsometry. At incubation times of 7200 min (120 h), ellipsometry shows hardly any increase in layer thicknesses caused by additional TFET adsorption, thereby once more indicating the formation of well-ordered SAMs.

In contrast, for sample **3a**, significantly different behavior is found. As already observed previously (cf. Figure 5), the native films become even slightly thinner for long incubation times (> 5 h). This decrease of the layer thickness could be rationalized by the disturbing effect of the hexyl side chains during the formation of the native film, causing a higher degree of structural defects. Therefore, during the post-adsorption of TFET, the molecules have more space to adjust and incline, which then may lead to the deliberation of adsorption sites for TFET. Therefore, in particular, for long incubation times, the post-adsorption experiment gives a significant increase in layer thickness due to TFET adsorption. This finding is in accordance with the poor SAM formation behavior of **3a**, as already revealed by the surface analysis.

Interestingly, the post-adsorption does not significantly change the contact angles (data not shown) for any of the three molecules, most likely because of the small size of the molecule, which is probably buried underneath the phenothiazine layer.

The exact amount of adsorbed TFET was determined from the intensity of the XPS F 1s peak, relative to that obtained from a complete monolayer of TFET on gold (see Figure 9b). Expectedly, the F 1s peak is observed at 686.8 eV. For sample **5b** the F 1s signal is fairly weak (6.9%). The film for sample **5a** has adsorbed more TFET (18.5%), and, finally, the film for sample **3a** contains a significant amount of fluorine (48.2%).

In Figure 9c, the relative peak area of the XPS F 1s signal of the three samples is plotted as a function of the incubation time of the substrates into the respective phenothiazine derivative solutions. For the films of sample **5b**, the amount of fluorine is very low, in comparison to that of the other two molecules, and even decreases with increasing incubation time, thus indicating almost-complete shielding of the surface, because of increased coverage and better ordering of this phenothiazine derivative, in corroboration of the surface analysis previously described. The films for sample **5a** show higher TFET adsorption, with only little dependence on the incubation time (the 300-min data point is apparently an outlier).

Chart 1. SAM of Thiolated Phenylethynyl Phenothiazines on Au{111}

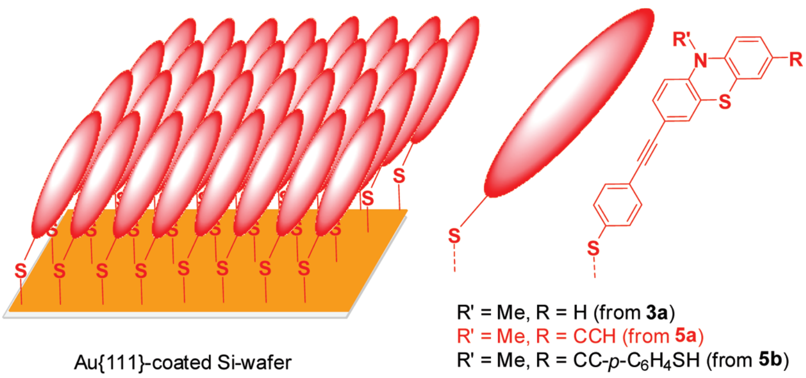

While the overall surface analysis of sample **5b** gave evidence for a well-ordered monolayer, the ellipsometry data (cf. Figure 5) in fact revealed saturation coverage slightly below the theoretical limit, which may explain the somewhat-higher TFET adsorption currently observed. In contrast to these basically promising results, the films for sample **3a** exhibit a significant increase in the fluorine content with increasing incubation time, thereby giving, once more, evidence for the poor monolayer formation of this molecule. Presumably, the **3a** molecules reorganize with increasing incubation time in such a way that even more adsorption places for TFET are generated than in the initial phase of film formation. A corresponding molecular rearrangement can also be observed in the IRRA spectra, in particular, for the region of the CH stretching vibrations (vide supra). Because the post-adsorption time for TFET was kept constant at 24 h in all cases, this scenario is more likely than desorption caused by TFET.

Conclusions

Sonogashira coupling of alkynyl (oligo)phenothiazines with 1-(*S*-acetylthio)-4-iodo benzene furnishes phenylethynyl phenothiazinyl thioacetates, which is a class of redox-active, fluorescent π-systems with acetyl-protected "alligator clips" for chemisorption to conductive gold surfaces. These thioacetates show reversible one-electron oxidations at relatively low oxidation potentials. The reversible oxidation behavior is maintained after in situ deprotection, leading to chemisorption on the electrode surface. After multisweep experiments, no traces of desorbed molecules can be detected in the electrolyte, indicating the formation of stable adsorbates. Furthermore, the oligomeric phenothiazinyl representatives reveal considerable greenish-blue luminescence with substantial fluorescence quantum yields and large Stokes shifts. Adsorption kinetics and structures of the formed monolayers of three 4-mercapto phenylalkynyl phenothiazinyl molecules on gold were investigated using several techniques. Ellipsometry shows that all molecules are forming films on gold within 300 min without multilayer formation. The final coverage of samples **5a** and **5b** on gold are in very good agreement with the calculated layer thicknesses, assuming an orthogonal orientation of the molecules on the surface. The sample film of compound **3a** reveals a deviation of almost 5 Å from the calculated values. The water contact angles of the layers of **5a** and **5b** on gold are consistent with literature values. For the layers of **3a** on gold, the higher contact angle of 90° can be attributed to the hydrophobic influence of the hexyl side chain. The stoichiometric ratios C 1s/S 2p of samples **5a** and **5b** on gold determined by XPS match very well with calculated data when a layer model is applied, thus yielding evidence for well-ordered layers with a well-defined orientation and alignment of the molecules. In contrast, the samples of **3a** on gold are better-described by a statistic model with an irregular orientation of the molecules on the surface.

In the IRRA spectra of sample **5a** on gold, the bands clearly indicate that the molecules are oriented close to the gold surface normal. The same bands are found in the spectra of sample **5b** on gold, and, in combination with the layer thicknesses determined by ellipsometry, evidence is given that this molecule is bound to the gold surface with only one S atom and that it is oriented orthogonally. In the CH-region of the spectra of sample **3a** on gold, the hexyl chain is clearly identified by four distinct aliphatic CH stretching vibrations. With increasing incubation times, these bands are diminishing, as a consequence of molecular reorientation with immersion of the hexyl chains into the phenothiazine layer and/or desorption of the **3a** molecules.

Post-adsorption studies with trifluoroethanthiol (TFET) show that the layers of sample **5a** form almost-perfect SAMs on gold (see Chart 1), where only 6.9% of the fluorine amount is post-adsorbed. The films of **5a** and **3a** insert fluorine amounts of 18.5% and even 48.2%. Hence, compound **3a** does not form close-packed films on gold, as a consequence of the disturbing hexyl side chain. The higher quality of the films of compound **5b** on gold is supposedly a consequence of the presence of two thiol groups, which increases the adsorption probability, despite the bulkiness of the molecule. This is a very interesting observation, since, a priori, it might have been expected that the molecule adsorbs with both thiol groups on the gold surface, thereby bridging between two different adsorption sites. The fact that this is not the case sheds light on the importance of the Au−S−C angle for SAM structure.[30] In addition, with the free thiol groups on top

(30) Rong, H. T.; Frey, S.; Yang, Y. J.; Zharnikov, M.; Buck, M.; Wuhn, M.; Woll, C.; Helmchen, G. *Langmuir* **2001**, *17*, 1582–1593.

of the monolayer, SAMs of **5b** promise to be ideal candidates for the formation of intermetal junctions and, thus, molecular diode fabrication.

In summary, our study reveals that phenothiazines with thioacetate functionalities are well-suited for SAM formation on gold electrodes and surfaces and, thus, are excellent candidate systems for the buildup of complex redox switchable ultrathin films for molecular electronics applications. Besides the high degree of order achieved, which warrants well-defined electronic and optical properties of the structures formed, one interesting aspect of the systems studied is related to the possibility of triggering the chemisorption process by the addition of ammonium hydroxide. This chemical trigger enables better control of film formation and adsorption kinetics, which can be very useful, for example, for coadsorption of the moieties with a second, nonconductive molecule, which shall serve as insulating matrix. Further studies directed toward such more-complex oligophenothiazine SAMs on gold and functionalized redox manipulable surfaces are currently underway.

Acknowledgment. This project was supported by the DFG (SFB 486) and the Fonds der Chemischen Industrie. S.S. and M.H. acknowledge gratefully partial support by the DFG under Hi 693/2-2.

Supporting Information Available: Analysis of the structure of SAMs formed from **3a**, **5a**, and **5b** by IRRAS. (PDF) This information is available free of charge via the Internet at http://pubs.acs.org/.